VARIFORC processing examples

Correction of positive mean fields

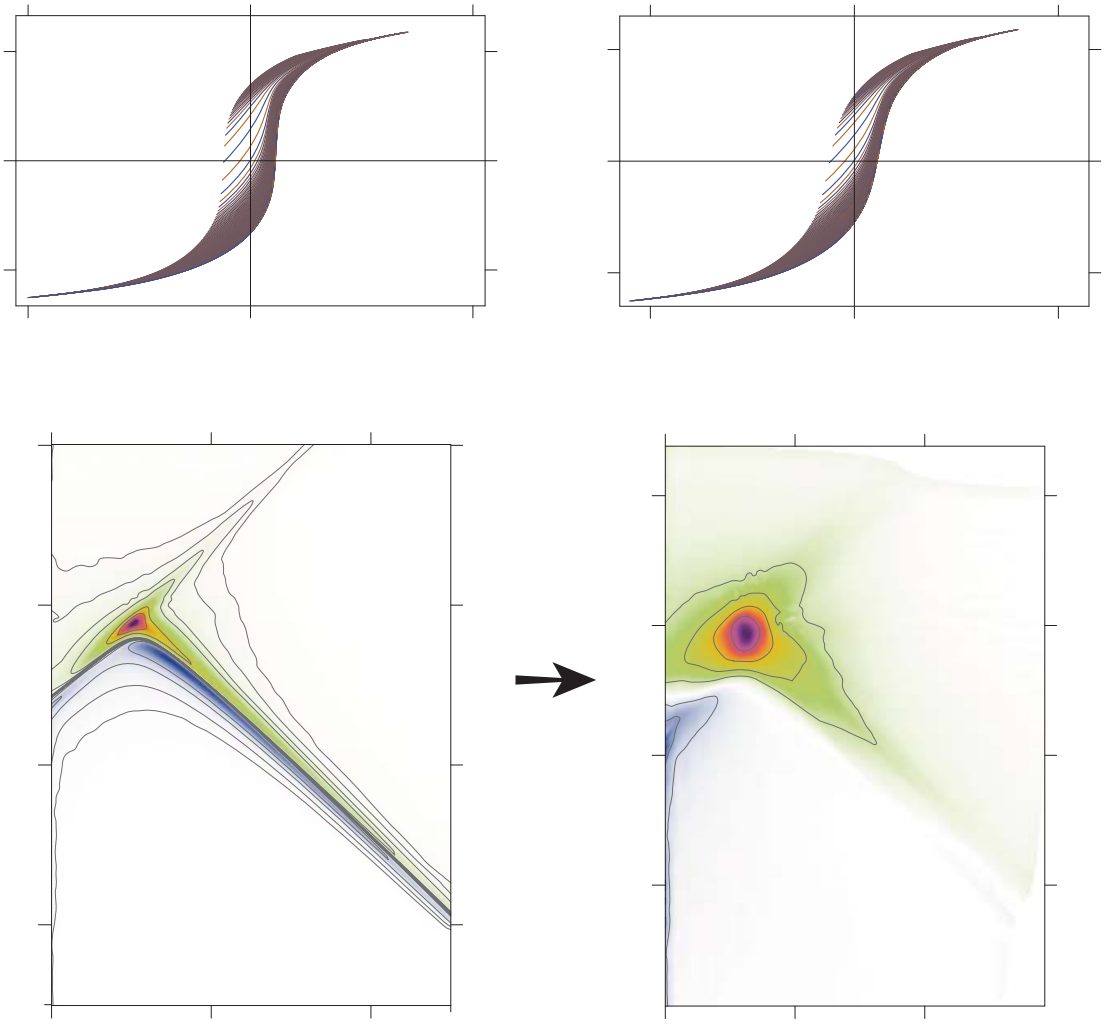

About this example

The measured material consists of a ~200 nm polycrystalline Fe film made of ~40 nm Fe grains (courtesy of John McCloy). This example handles FORC processing aspects related to rectangular hysteresis loops shaped by strongly magnetizing internal fields, and how the effects of such fields can be corrected so that "intrinsic" properties depending exclusively on applied fields are represented by the FORC diagram.

In general, an additional, so-called *internal field* exists inside the sample being measured. Internal fields are produced by the sample itself and can always be expressed as the sum of a local, random component (e.g. in disordered magnetic particle dispersions), and a component that is proportional to the bulk magnetization (e.g. demagnetizing fields). The latter component is often referred to as a *mean field*. While random internal fields "blur" the intrinsic FORC signature of the material being measured, mean fields introduce additional features to the FORC diagram, which are unrelated to intrinsic material properties. These features depend on the sign of the proportionality constant linking the mean interaction field with the bulk magnetization: *positive mean fields* and *negative mean fields* are characterized by positive and negative constants, respectively. This example deals with positive mean fields, i.e. fields that tend to reinforce existing magnetizations inside the specimen being measured. The reinforcement action tend to produce rectangular hysteresis loops, as shown in this example.

FORC measurements

- Measuring instrument: PMC MicroMag 2900 VSM.
- Specimen preparation: Unknown.
- FORC measurement protocol:

```
Hc1 = 0      , Hc2 = 0.05 T
Hb1 = -0.05 T, Hb2 = +0.02 T
Hsat = 1 T
Averaging time       = 0.1 s
Pause at calibration = 1 s
Pause at reversals   = 1 s
Pause at saturation  = 2 s
Smoothing = 1 (adds a 1-point margin to the measured range)
```

- Derived measurement parameters:

```
Number of curves: 485
Calibration measurements at 0.071 T
Mean size of field steps = 0.25 mT (maximum resolution of the FORC diagram)
```

- **Notes on measurements.** None

About VARIFORC processing options used in this example

VARIFORC modules are controlled by processing options stored in so-called parameter files. Parameter files used to process FORC data related to this example can be find in the folder containing this document. These are:

1. Import and correct FORC measurements (`ImportFORC` module):

- `PolyFe_VARIFORC_ImportFORC_parameters.txt`: import FORC data with first-point correction. Error calculation is disabled (`INPUT 10` set to 1), because it would just reflect smoothing artifacts on parts of the curves with extremely large slopes. The only effect of this processing option is that outliers – which are in any case absent in this set of measurements – cannot be detected. The high-field susceptibility (`INPUT 19`) has been set to 0 because the specimen does not contain para- or diamagnetic contributions.

2. Calculate the FORC diagram (`CalculateFORC` module):

- `PolyFe-SF1.5_VARIFORC_CalculateFORC_parameters.txt`: conventional processing with a constant smoothing factor (SF = 1.5). For demonstration purposes only.
- `PolyFe-vari_VARIFORC_CalculateFORC_parameters.txt`: optimized variable smoothing with smoothing factor limitations along diagonals with maximum first derivatives.
- `PolyFe-mfc-initial_VARIFORC_CalculateFORC_parameters.txt`: same as previous, with an initial mean field correction (`INPUT 17`: constant smoothing factor of 1 used for the calculation of M, and α = +0.25 mAm^2/T) at low resolution (`INPUT 06` set to `Coarse`).
- `PolyFe-mfc-final_VARIFORC_CalculateFORC_parameters.txt`: same as previous, with the final mean field correction (`INPUT 17`: constant smoothing factor of 1 used for the calculation of M, and α = +0.4 mAm^2/T) at full resolution (`INPUT 06` set to `0.00025`).

Low- and high-resolution measurements

The sample's hysteresis loop is characterized by extremely steep branches (Plates 1) and represents a limit example of rectangular hysteresis with associated FORC processing difficulties (see VARIFORC example on this topic). An important characteristics of FORC measurements associated with rectangular hysteresis is the tendency of the measured curve to accumulate near the upper and lower branches of the major hysteresis loop, so that the loop area is crossed only by few curves. Plates 1a,b show a "typical" FORC dataset with 73 curves measured in steps of ~2 mT: the largest gap between consecutive curves is almost as large as the saturation remanence. Poor resolution becomes evident in plots where the lower branch of the hysteresis loop has been subtracted from each curve (Plate 1b). In this case, the sharp peaks centered at ~14 mT are covered by only 4 measurement points. A much higher resolution is required for the correct calculation of corresponding features in the FORC diagram.

FORC difference plots like Plate 1b are part of the standard VARIFORC output and enable closer examination of important details that are not visible in conventional plots (e.g., Plate 1a). The envelope of curves from which the lower branch of the hysteresis loops has been subtracted coincides with the even component of the hysteresis loop, i.e. the difference between upper and lower branches [*Fabian and Dobeneck*, 1997].

High-resolution FORC measurements (485 curves measured in steps of 0.25 mT) have been used to cover the hysteresis loop area with a sufficient number of curves and adequately sample sharp magnetization changes (Plates 1c,d). Even so, the maximum gap between consecutive curves reaches 10% of the saturation remanence. Persistence of the ~14 mT peaks in Plate 1d in all curves is due to the fact that the chosen measurement protocol does not cover the whole hysteresis up to saturation: curves starting at larger negative field would display smaller peaks until full disappearance once measurements coincide with the lower branch of hysteresis.

Close inspection of the measured curves (Plates 1a,c), and, most importantly, of FORC difference plots (Plates 1b,d), enables a first verification of the chosen protocol. Insufficient coverage is manifested by difference curves that do not approach zero (for this purpose, the `INPUT 21` option of the **`ImportFORC`** must be set to `Hysteresis`, see the parameter file `PolyFe_VARIFORC_ImportFORC_parameters.txt`). On the other hand, characteristic features of the measured curves, such as rapid changes in slope and the peaks of Plate 1d should be covered by >10 measurements, and even more in case of visible measurement noise.

As in most VARIFORC examples, the first measurement point of all curves is affected by the sudden field sweep reversal preceding each curve. In most cases, first points lie slightly above the curve trend defined by the next points (see the VARIFORC example on first-point correction). This problem should not be confused with magnetic viscosity effects, which involve more points and is most pronounced for curves starting from the negative coercive field [*Pike et al.*, 2001]. First-point artifacts are corrected by replacing the affected measurements with a polynomial extrapolation of next points.

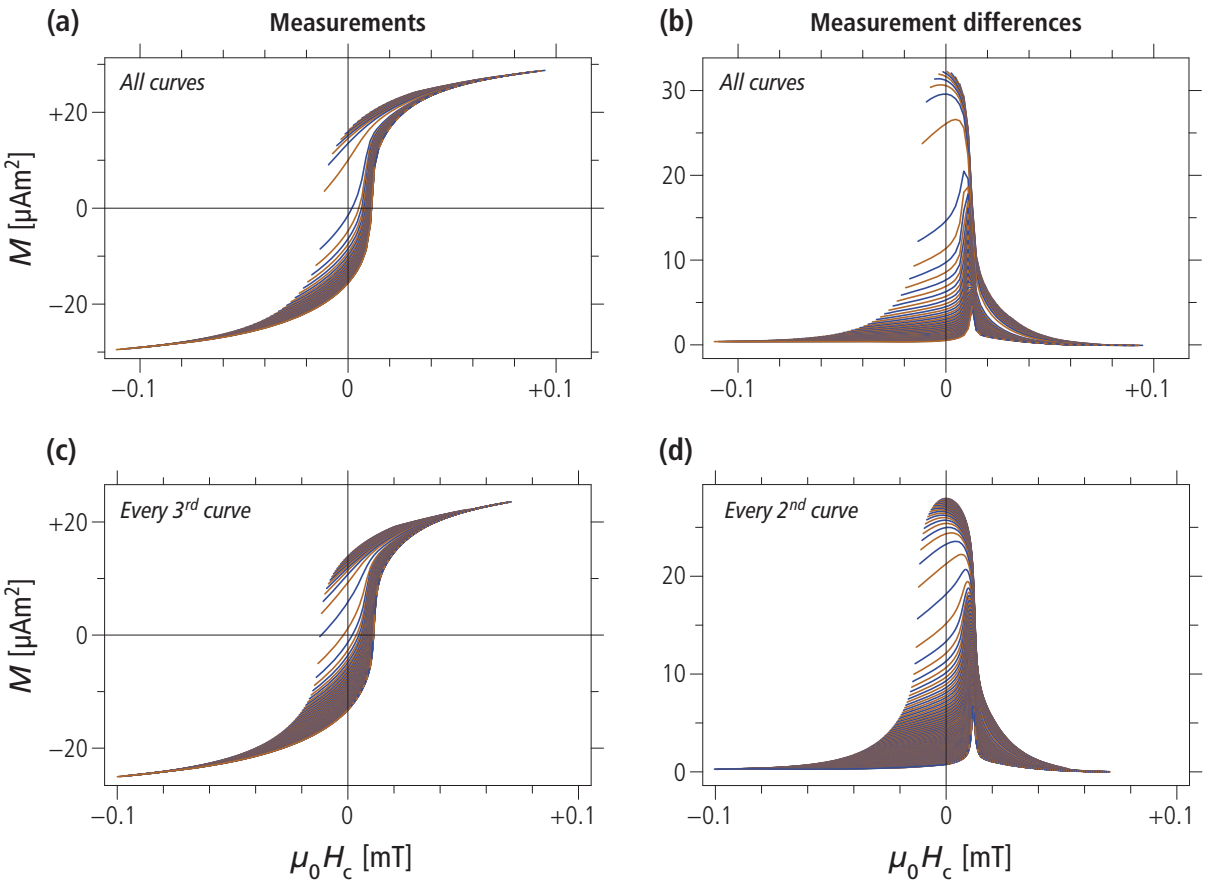

Plate 1. FORC measurements of a polycrystalline Fe film. Left plots show the measured curves after drift and outlier correction. Right plots show the same measurements after subtraction of the lower hysteresis branch reconstructed from the FORC measurements. **(a-b)** Low-resolution measurements (73 curves with ~2 mT field steps). Notice the large gaps between consecutive curves and poor resolution of the peaks in (b). **(c-d)** High-resolution measurements (485 curves with ~0.25 mT field steps). Every 3rd curve in (c) and every 2nd curve in (d) are shown for clarity. All plots were generated by **`ImportFORC`** with minor editing (see the parameter file `PolyFe_VARIFORC_ImportFORC_parameters.txt`).

FORC processing problems related to rectangular hysteresis

Rectangular hysteresis loops, as the one in this example, are characterized by particular FORC signatures requiring high-resolution measurements (see previous section) and special processing strategies in order to avoid smoothing artifacts. FORC processing difficulties are caused by rapid magnetization changes in proximity of the positive and negative coercive fields (Plate 2a). In FORC space, these changes are concentrated along two diagonals characterized by very large first derivatives $\partial M/\partial H_r$ and $\partial M/\partial H$, where H_r is the so-called reversal field at which curves begin, and H the field applied during measurements (Plate 2b). FORC diagram contributions are almost exclusively concentrated along these two diagonals, with the central peak located at the crossing point (Plate 2c). First derivative peaks along such diagonals, however, are not always associated with corresponding contributions in the FORC diagram, as seen with the VARIFORC rectangular hysteresis example based on non-interacting single-domain particles. The FORC signature shown here is caused by strongly magnetizing (positive) interactions.

FORC processing problems related to very large first derivatives are clearly identifiable on plots of the estimated FORC standard error (Plate 2d): maximum errors partially exceed corresponding FORC amplitudes along the diagonals, so that the FORC diagram in Plate 2c is not entirely significant. Error peaks raising above the mean measurement error are caused by polynomial regression artifacts over regions characterized by rapid magnetization changes, i.e. the two diagonals with maximum first-order derivatives. Conventional FORC processing with a constant smoothing factor, as in Plate 2c, is intrinsically inadequate, because regression artifacts can be reduced only upon decreasing the smoothing factor, at cost less efficient measurement error suppression. In this example, even a smoothing factor of 1.5 – which is usually inapplicable to weak natural samples – is not sufficiently small to completely eliminate regression artifacts, so that parts of the FORC diagram remain intrinsically insignificant.

FORC processing problems related to rectangular hysteresis can be solved with VARIFORC, as explained in the next section.

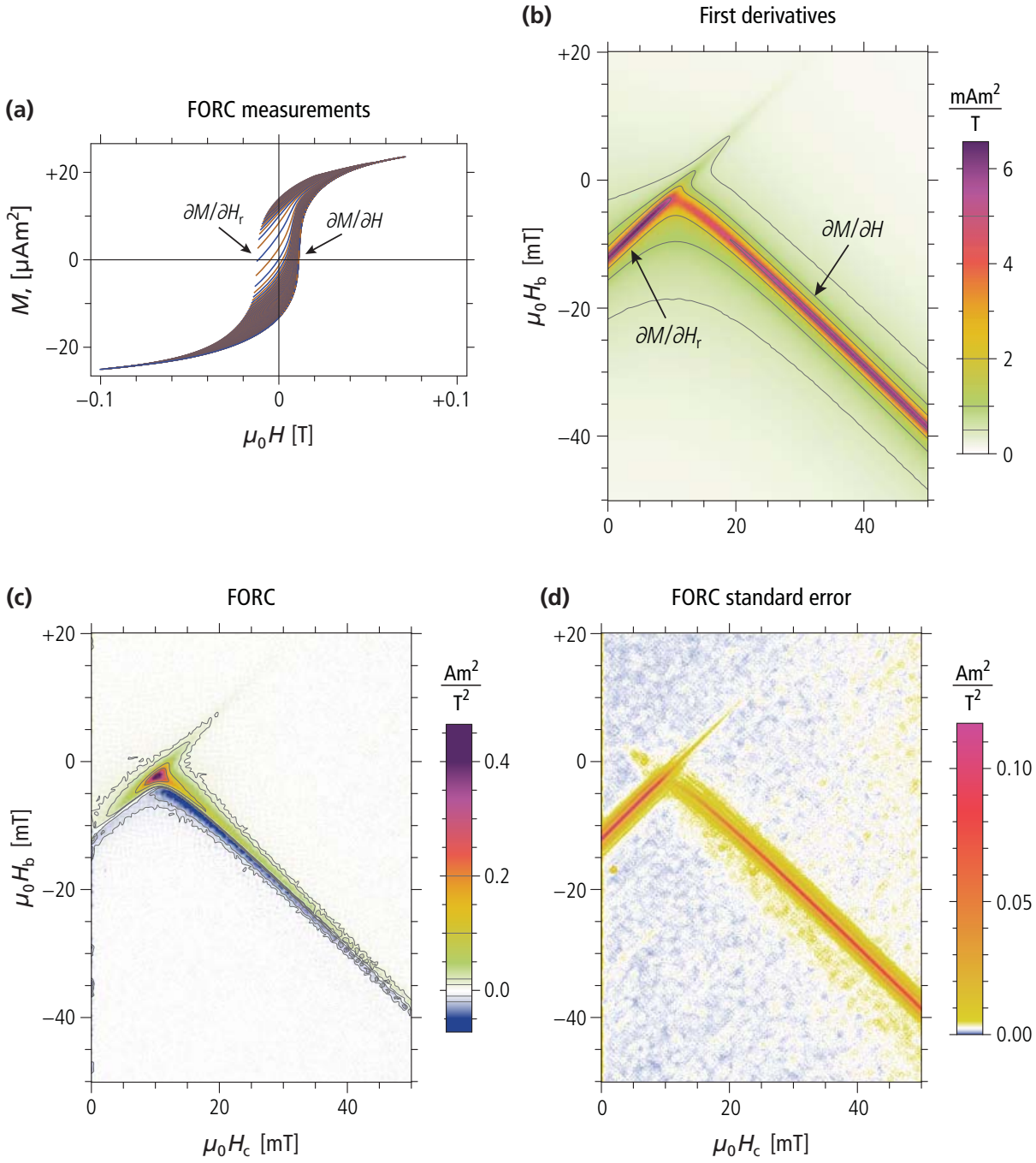

Plate 2. FORC processing problems related to rectangular hysteresis. (a) FORC measurements as in Plate 1c. Places with maximum first derivatives ($\partial M/\partial H_r$, corresponding to curve separation, and $\partial M/\partial H$, corresponding to curve slope) are indicated by arrows. **(b)** Plot of the total first derivative $\partial M/\partial H_r + \partial M/\partial H$ in FORC space. Contributions of $\partial M/\partial H_r$ and $\partial M/\partial H$ are concentrated along the ascending diagonal defined by $H_r = -H_{coerc}$ and the descending diagonal defined by $H = +H_{coerc}$, respectively, where H_{coerc} is the coercive field. **(c)** FORC diagram calculated with a constant smoothing factor SF = 1.5 (see `PolyFe-SF1.5_VARIFORC_CalculateFORC_parameters.txt`). **(d)** Estimated standard error of the FORC diagram shown in (c). The color scale is chosen so, that the root mean square error is plotted in white, smaller errors in blue, and larger errors in yellow and red. Peak errors along the maximum derivative diagonals partially exceed corresponding FORC amplitudes in (c).

VARIFORC processing

The FORC processing problems discussed in the previous section can be solved with a correct choice of measurement point arrays used for local polynomial regression. Usually, such arrays coincide with square [*Pike et al.*, 1999] or circular [*Harrison and Feinberg*, 2008] selections from the original measurement grid, which produce the same isotropic smoothing over the whole FORC space. Sometimes, however, different smoothing strengths are required at different places in the FORC diagram and along different directions: for example, highest resolution, and therefore minimum smoothing, is needed *across* the diagonals with large FORC contributions in Plate 3b, while the opposite applies *along* the same diagonals. On the other hand, strong smoothing can be applied to the remaining parts of the diagram.

VARIFORC addresses different smoothing needs by defining the size of measurement point selections along directions defined by the upright FORC coordinate system (i.e., along H_c and H_b) as well as the 45°-rotated measurement coordinates (i.e., along H_r and H). For example, a linear increase of the smoothing factor, proportionally to the distance from $H_c = 0$ and $H_b = 0$, respectively, is justified by Preisach models of the FORC function [*Preisach*, 1935], and is realized with upright rectangular selections of measurement points [*Egli*, 2013]. On the other hand, smoothing requirements along diagonals of the FORC space are handled by rectangular selections that are rotated by 45°. The two systems are merged by intersecting upright and rotated selections, as seen in Plate 3d. In this example, the size of measurement selections is smallest across the diagonals defined by $H_r = -H_{coerc}$ and $H = +H_{coerc}$, where, as seen in the previous section, first derivatives are maximal. These diagonals are automatically located by VARIFORC, and the user is only required to enter the maximum smoothing factor allowed across them, which, in this example, is 1.5 (see `INPUT 14` in the parameter file `PolyFe-vari_VARIFORC_CalculateFORC_parameters.txt`).

The FORC diagram obtained with the processing strategy illustrated above (Plate 3e) contains much finer details than the conventional counterpart (Plate 3b), and, most importantly, all its features are significant at a 95% confidence level (which corresponds to a signal-to-noise ratio >3, see Plate 3f).

Boomerang-shaped, negative FORC amplitudes below the central maximum (Plate 3e) represent a characteristic signature of a magnetizing mean internal fields, which reinforce the field applied during the measurements. Because such mean fields are proportional to the sample magnetization, a nonlinear relation exists between the applied field on one hand, and the total field "seen" by the magnetic material inside the specimen on the other hand. Accordingly, the "intrinsic" FORC properties of the measured material are not necessarily reflected by the measured FORC diagram, as it is the case in this example. VARIFORC can correct such effects, as explained in the next sections.

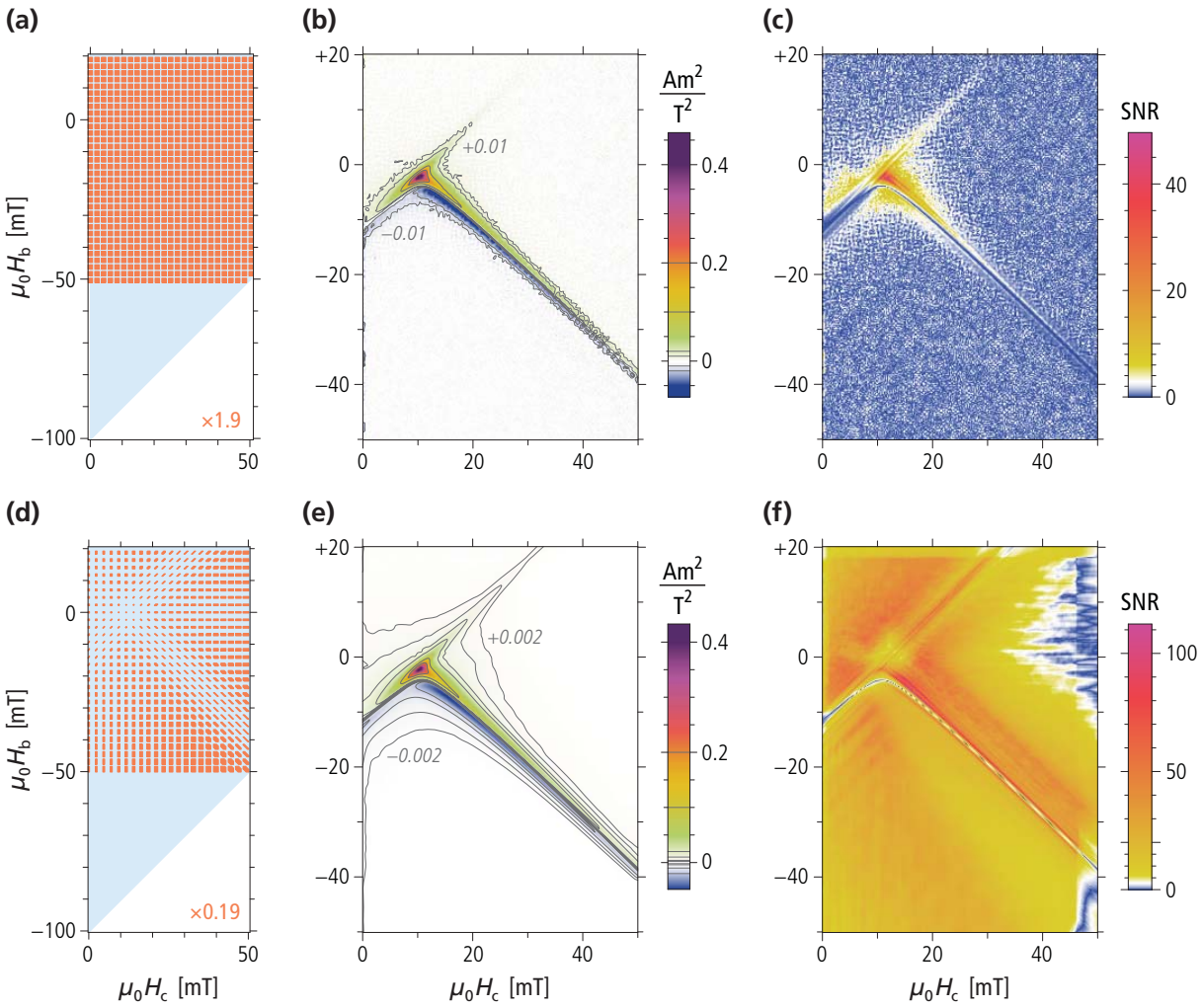

Plate 3. Comparison between conventional and VARIFORC processing. Left plots: Rectangular selections (orange, not to scale) of measurement points (shaded blue area) used for polynomial regression. The size of these rectangular selection is controlled by a horizontal (s_c) and a vertical (s_b) smoothing factor, and, along diagonals, by an additional pair s_r, s_d of smoothing factors. **Middle plots:** FORC diagrams calculated with polynomial regression over measurement point arrays shown in the left plots. **Right plots:** Signal-to-noise (SNR) ratios of the FORC diagrams shown in the middle plots, calculated on the basis of the estimated standard error of regression. The color scale is chosen so, that the threshold for significant FORC contributions (i.e. SNR ≈ 3 at a 95% confidence level) is plotted in white. Accordingly, significant regions of the FORC diagram correspond to yellow, red, and purple regions. **(a-c)** Conventional processing with a constant smoothing factor SF = 1.5 (i.e. $s_c = s_b = 1.5$, see the parameter file `PolyFe-SF1.5_VARIFORC_CalculateFORC_parameters.txt`). Numbers in (b) show the smallest contour level. Only a small region of the FORC diagram around the central peak is significant according the SNR plot in (c). **(d-f)** Advanced FORC processing with smoothing factors increasing towards large H_c- and H_b-amplitudes, and limitations to SF = 1.5 across the diagonals defined by maximum first derivatives (see the parameter file `PolyFe-vari_VARIFORC_CalculateFORC_parameters.txt`). Numbers in (d) show the smallest contour level. The whole FORC diagram is significant, as shown in (f), except for a thin stripe corresponding to places where the FORC function changes its sign and is forced to pass through zero amplitudes, which are by definition not significant. The smallest contour level in (e) corresponds to 0.5% of the maximum FORC amplitude and is still significant.

Internal mean fields

Magnetic hysteresis, including related FORC measurements, is controlled by the total magnetic field H_{tot} inside the specimen, rather than the externally applied field H. The total field is the vector sum of the applied field and an internal field, H_i, which originates from the specimen's magnetization $M(H)$, i.e. $\mathbf{H}_{tot} = \mathbf{H} + \mathbf{H}_i$. The relation between internal field and magnetization is very complex. Some magnetic configurations with no net magnetic moment (Plate 4a,b) do not produce any internal field, while volumes carrying a net magnetic moment, such as the homogeneously magnetized parallelepiped in Plate 4c, produce a non-zero internal field, as well as an external field, which, at greater distance, converge to that of the equivalent dipole moment.

The internal field of homogeneously magnetized bodies is always opposed to the magnetization and is therefore often referred to as the *demagnetizing field* H_d [*Coey*, 2010]. Although H_d depends in general on the position inside the magnetized body (Plate 4c), it is often conveniently approximated by the homogeneous demagnetizing field of ellipsoidal bodies (Plate 5). This field is given by $\mathbf{H}_d = -\mathbf{N}\cdot\mathbf{M}$, where $\mathbf{N}$ is the so-called *demagnetizing tensor*, with principal components N_x, N_y, and N_z controlled by the principal axes of the ellipsoid [*Osborn*, 1945]. In general, the demagnetizing factor is largest along the shortest axis and vice-versa, with $N_x = N_y = N_z = 1/3$ for a sphere.

Another internal field source is found in heterogeneous materials, in particular those consisting of magnetic particles dispersed in a non-magnetic matrix. In this case, each particle produces a magnetic field that affects the other particles in what is known as *magnetostatic interactions*. The total field produced by all particles at a given point inside the specimen is called *magnetostatic interaction field*, $\mathbf{H}_{int}$. For modelling purposes, the interaction field is often divided into a random component, which depends on the local configuration of near particles, and a mean component which arises from direction-dependent interparticle distances. In isotropic samples (Plate 6a), there is not a particular direction with shortest or largest distances, and the mean value of $\mathbf{H}_{int}$ is zero. In textured samples featuring oriented "chains" of magnetic particles (Plate 6b), the mean interaction field is parallel to the particle's magnetic moments and has a reinforcing effect on the existing magnetization. It is therefore called *magnetizing*, or *positive* interaction field. On the other hand, magnetic particles organized in sheets that are perpendicular to the applied field experience the opposite effect of a mean interaction field that is antiparallel to the magnetic moments (Plate 6c). This field is called *demagnetizing*, or *negative* interaction field. In analogy with demagnetizing fields, the mean interaction field is given by $\mathbf{H}_{int} = \mathbf{S}\cdot\mathbf{M}$, where $\mathbf{S}$ is a tensor expressing particle distance anisotropies. Unlike the demagnetizing tensor, $\mathbf{S}$ can yield positive as well as negative mean interaction fields, depending on the angle between magnetization and the principal axes of $\mathbf{S}$.

In general, distribution anisotropy imparts a net anisotropy to the whole sample [*Stephenson*, 1994], unless the specimen is divided into microscopic sub-volumes characterized by randomly oriented distribution anisotropy tensors. In such cases, distribution anisotropy contributions of individual sub-volumes do not cancel out completely: magnetic particles arranged in chains will bear the signature of a positive net interaction field, while the opposite occurs with sheet arrangements. In this case, the mean interaction field is given by $\mathbf{H}_{int} = S\mathbf{M}$, where S is a positive or negative scalar.

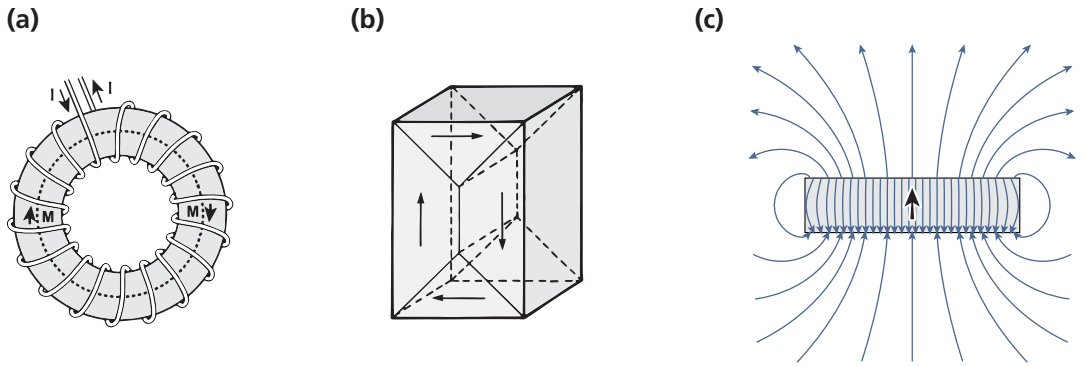

Plate 4. Magnetizations and internal fields. (a-b) Magnetized bodies with no net magnetic moment, which do not generate any internal or external magnetic field. **(a)** Toroidal magnetic core, whose toroidal magnetization *M* is induced by the electric current *I* flowing around the core. **(b)** Four magnetic domain in a parallelepiped with cubic magnetocrystalline anisotropy. **(c)** A homogeneously magnetized plate (magnetization parallel to the black arrow) generates inhomogeneous internal and external fields (blue lines).

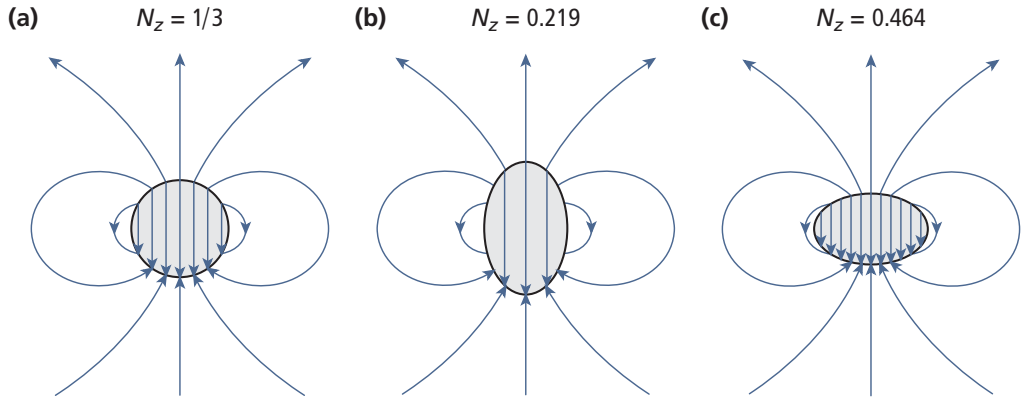

Plate 5. Fields produced by homogeneously magnetized ellipsoids. Ellipsoid are rotation-symmetric about the vertical. N_z is the vertical principal component of the demagnetizing tensor. **(a)** Sphere ($N_x = N_y = N_z = 1/3$). **(b)** Prolate ellipsoid with 2:1 axis ratio. The limit case of a needle yields $N_z = 0$ and $N_x = N_y = 1/2$. **(c)** Oblate ellipsoid with 1:2 axis ratio. The limit case of a thin sheet yields $N_z = 1$ and $N_x = N_y = 0$.

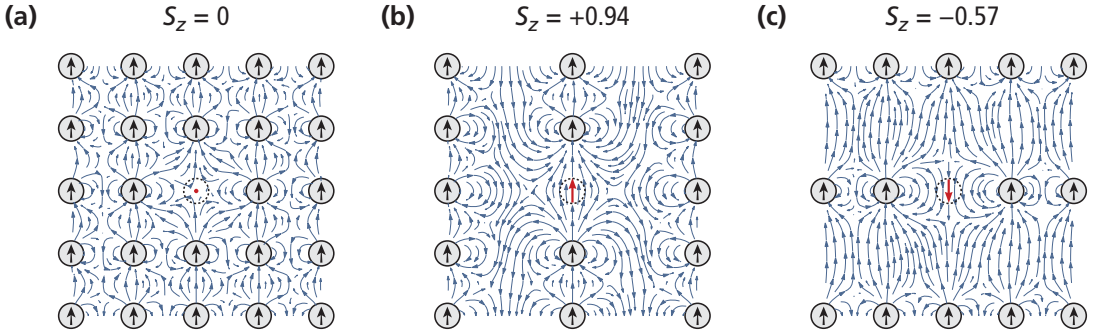

Plate 6. Distribution anisotropy examples. Magnetic particles (gray with magnetic moments indicated by arrows) are arranged on prismatic lattices. The interaction field is shown by blue lines, and, at the place of the middle particle, by a red arrow. **(a)** Particles on a cubic lattice have no distribution anisotropy. **(b)** Particle "chains" along z produce a positive mean interaction field. **(c)** Particle "sheets" perpendicular to z produce a negative mean interaction field.

Mean field correction

As seen in the previous section, the total field inside a specimen is, on average, given by

$$\mathbf{H}_{tot} = \mathbf{H} + (\mathbf{S} - \mathbf{N}) \cdot \mathbf{M}(\mathbf{H}) \quad (1)$$

where $\mathbf{H}$ is the applied field, $\mathbf{M}$ is the specimen magnetization, $\mathbf{N}$ is the demagnetizing tensor related to the specimen shape, and $\mathbf{S}$ is the distribution anisotropy tensor related to the texture of dispersed magnetic particles. Although $\mathbf{H}_{tot}$ is not necessarily parallel to the applied field, its effects can be approximated by considering its component parallel to $\mathbf{H}$, in which case equation (1) becomes

$$H_{tot} = H + \alpha M(H) \quad (2)$$

with $\alpha = S - N$ being a scalar correction factor and $M(H)$ the measured magnetization. If measured magnetization curves are defined by points with coordinates (H, $M(H)$), *intrinsic magnetization curves* are simply defined through equation (2) as (H_{tot}, $M(H)$). The calculation of such intrinsic curves is called *mean field correction*, and can be applied to any type of magnetic measurements, including FORCs. Depending on the sign of α, a main distinction is made between *positive mean field corrections* (i.e., $\alpha > 0$), and *negative mean field corrections* (i.e., $\alpha < 0$). Because α is generally unknown, mean field corrections of FORC measurements are of empirical nature. Typically, a positive or negative starting value of α is chosen, depending on suspect mean field signatures recognized in the uncorrected FORC diagram. In this example, the FORC diagram is dominated by strong positive mean field signatures, in form of boomerang-shaped negative amplitudes below the central maximum (Plate 6b). Therefore, a positive α is chosen.

Because demagnetization and distribution anisotropy tensors are defined on the basis of volume-normalized magnetizations (SI unit: A/m, cgs unit: emu/cm^3) and proper magnetic field units (SI unit: A/m, cgs unit: Oe), the initial choice of α depends on conversion of intrinsic tensor values into the unit system used for the FORC measurements. If such conversion is not possible – for instance because the sample volume is unknown, as in this example –suitable initial choices of α are given by fractions of $\pm M_s/H_{sat}$, where M_s is the saturation magnetization and H_{sat} is the saturation field, i.e. the field in which the hysteresis loop becomes closed. Both M_s and H_{sat} are expressed in the same units of the imported data, as specified in the file header. In this example, $M_s \approx 0.03$ mAm^2 and $H_{sat} \approx 0.06$ T (Plate 6a, the magnetization unit of the source data is mAm^2 instead of µAm^2), so that a possible initial guess is given by 50% of $M_s/H_{sat} \approx 0.5$, i.e. $\alpha = 0.25$. Caution should be used with this initial step, in order to avoid overcorrections.

Once the first mean-field-corrected FORC diagram is calculated, α is adjusted in successive steps until the original mean field signatures are completely removed, or signatures from mean fields with opposed sign start to appear. For this purpose, FORC diagrams can be calculated at a lower resolution (see `INPUT 06` in the parameter file `PolyFe-mfc-initial_VARIFORC_CalculateFORC_parameters.txt`), until a satisfactory result is obtained – in this example by choosing $\alpha = 0.4$ (Plate 6d). The corrected FORC diagram bears the typical signature of strongly interacting single-domain particles [*Carvallo et al.*, 2005], which is compatible with ~40 nm Fe particles. As seen from the vertical spread of the diagram, random interaction fields are not removed by mean field corrections.

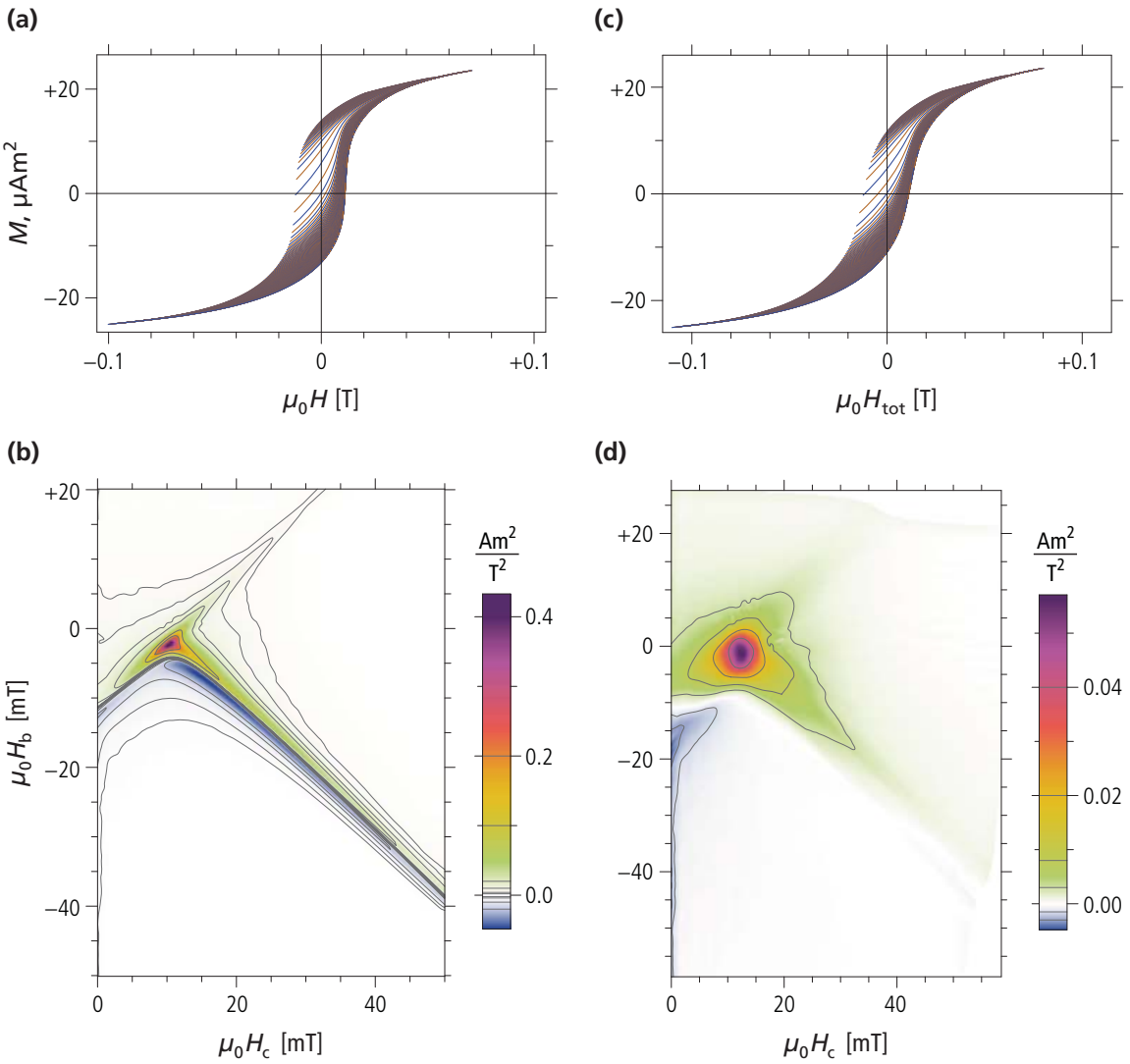

Plate 6. Positive mean field correction. (a) Original drift- and outlier-corrected FORC measurements, as in Plate 1. **(b)** FORC diagram calculated from measurements in (a), as in Plate 3. Boomerang-shaped negative amplitudes below the central maximum are a typical signature of a positive mean field. **(c)** Same as (a), after a mean field correction with α = +0.4 mAm^2/T. The hysteresis loop formed by the corrected curve envelope has now much less steep flanks. **(d)** FORC diagram calculated from measurements in (c). Smoothing parameters are identical to those used in (b), because the selection of measurement points for local polynomial regression is performed in the uncorrected FORC space defined by measurement coordinates. The only difference to the parameter file used in (b) is the definition of a smoothing factor used to fit the magnetization curves (in this case, 1) and the mean field correction factor (in this case, 0.4). These parameters are entered with `INPUT 17` (see the parameter file `PolyFe-mfc-final_VARIFORC_Calculate FORC_parameters.txt`). The positive mean field signature is not completely removed, as seen from residual contributions along diagonals departing from the central maximum. However, larger values of α produce new artifacts corresponding to the signature of negative mean fields, so that α = +0.4 mAm^2/T is the best mean field correction that can be applied in this case. The persistence of residual mean field signatures can be explained by the fact that a proper correction would require vector calculations according to equation (1). Furthermore, different mean fields might be applicable to specimen sub-volumes. Nevertheless, the typical signature of interacting single domain particles is now clearly visible (random interaction fields are not affected by mean field correction).

Literature

Carvallo, C., D.J. Dunlop, Ö. Özdemir (2005). Experimental comparison of FORC and remanent Preisach diagrams, *Geophysical Journal International 162*, 747-754.

Coey, J.M.D. (2010). *Magnetism and Magnetic Materials*, Cambridge University Press, Cambridge.

Egli, R. (2013). VARIFORC: An optimized protocol for calculating non-regular first-order reversal curve (FORC) diagrams, *Global and Planetary Change 110*, 302-320, doi:10.1016/j.gloplacha.2013.08.003.

Fabian, K., T. von Dobeneck (1997). Isothermal magnetization of samples with stable Preisach function: A survey of hysteresis, remanence, and rock magnetic parameters, *Journal of Geophysical Research 102*, 17659-17677.

Harrison, R.J., and J.M. Feinberg (2008). FORCinel: An improved algorithm for calculating first-order reversal curve distributions using locally weighted regression smoothing, *Geochemistry, Geophysics, Geosystems 9*, Q05016, doi:101029/2008GC001987.

Osborn, J.A. (1945). Demagnetizing factors of the general ellipsoid, *Physical Review 67*, 351-357.

Pike, C.R., A.P. Roberts, K.L. Verosub (1999). Characterizing interactions in fine magnetic particle systems using first order reversal curves, *Journal of Applied Physics 85*, 6660-6667.

Pike, C.R., A.P. Roberts, K.L. Verosub (2001). First-order reversal curve diagrams and thermal relaxation effects in magnetic particles, *Geophysical Journal International 145*, 721-730.

Preisach, F. (1935). Über die magnetische Nachwirkung, *Zeitschrift für Physik*, *94*, 277-302.

Stephenson, A. (1994). Distribution anisotropy: Two simple models for magnetic lineation and foliation, *Physics of the Earth and Planetary Interiors 82*, 49-53.